

High power (60 mW) GaSb-based 1.9 μm superluminescent diode with cavity suppression element

Nouman Zia, Jukka Viheriälä, Riku Koskinen, Antti Aho, Soile Suomalainen, and Mircea Guina

Citation: *Appl. Phys. Lett.* **109**, 231102 (2016); doi: 10.1063/1.4971972

View online: <http://dx.doi.org/10.1063/1.4971972>

View Table of Contents: <http://aip.scitation.org/toc/apl/109/23>

Published by the [American Institute of Physics](#)

Articles you may be interested in

[III-Nitride-on-silicon microdisk lasers from the blue to the deep ultra-violet](#)

Appl. Phys. Lett. **109**, 231101 (2016); 10.1063/1.4971357

[Temperature invariant energy value in LED spectra](#)

Appl. Phys. Lett. **109**, 231103 (2016); 10.1063/1.4971831

[Terahertz master-oscillator power-amplifier quantum cascade lasers](#)

Appl. Phys. Lett. **109**, 231105 (2016); 10.1063/1.4969067

[Incorporation of gold into silicon by thin film deposition and pulsed laser melting](#)

Appl. Phys. Lett. **109**, 231104 (2016); 10.1063/1.4971358

High power (60 mW) GaSb-based 1.9 μm superluminescent diode with cavity suppression element

Nouman Zia,^{a)} Jukka Viheriälä, Riku Koskinen, Antti Aho, Soile Suomalainen, and Mircea Guina

Optoelectronics Research Centre, Tampere University of Technology, Tampere FIN-33101, Finland

(Received 27 September 2016; accepted 26 November 2016; published online 6 December 2016)

The characteristics and the fabrication of a 1.9 μm superluminescent diode utilizing a cavity suppression element are reported. The strong suppression of reflections allows the device to reach high gain without any sign of lasing modes. The high gain enables strong amplified spontaneous emission and output power up to 60 mW in a single transverse mode. At high gain, the spectrum is centered around 1.9 μm and the full width at half maximum is as large as 60 nm. The power and spectral characteristics pave the way for demonstrating compact and efficient light sources for spectroscopy. In particular, the light source meets requirements for coupling to silicon waveguides and fills a need for leveraging to mid-IR applications photonics integration circuit concepts exploiting hybrid integration to silicon technology. © 2016 Author(s). All article content, except where otherwise noted, is licensed under a Creative Commons Attribution (CC BY) license (<http://creativecommons.org/licenses/by/4.0/>). [<http://dx.doi.org/10.1063/1.4971972>]

Semiconductor light sources emitting in the mid-infrared spectral region (2–4 μm) are becoming increasingly appealing for gas sensing as well as medical and defense applications. In particular, gas sensing takes advantage of the presence of numerous absorption lines for gases such as methane, ozone, carbon dioxide, and carbon monoxide.¹ This has led to intensified research on the development of different semiconductor laser sources for this spectral range, covering both InP² and GaSb^{3–5} material systems. While laser diodes typically emit high output powers and can exhibit single wavelength operation, the tunability of the spectrum is rather small, and therefore several light sources operating with different wavelengths are required to be able to simultaneously measure different gases. On the other hand, superluminescent diodes (SLDs) offer a unique combination of optical characteristics including high brightness, good beam directionality, low temporal coherence, and a broad emission spectrum. A single SLD operating at this wavelength range could be applied for monitoring multiple gases simultaneously. Previously, SLD development has focused on near infrared ($\lambda < 2 \mu\text{m}$) wavelengths exploiting mainly InP-based emitters,⁶ while the GaSb-based SLDs have not raised much attention. Thus, the performance of SLDs for 2–3 μm spectral range has not met the demands of sensing applications due to very low output powers.^{7,8} Recent demonstration in this area includes continuous wave (CW) operation of SLDs at room temperature (RT) with output powers up to 40 mW at 2.05 μm and 5 mW at 2.38 μm .⁹

Here, we report a GaSb-based single-transverse mode SLD emitting at $\sim 1.9 \mu\text{m}$ with a maximum output power of ~ 60 mW. The output-power represents a 50% improvement compared to the recent results on the GaSb-based long-wavelength SLD.⁹ At room-temperature, the SLD has a spectral full-width at half maximum (FWHM) of 60 nm. These results

are enabled by the use of GaInSb quantum wells (QWs) placed in a long waveguide, which provide strong material gain and strong amplified spontaneous emission (ASE). Preliminary observations indicated that when using conventional fabrication techniques, the output power for SLDs operating in this wavelength range is limited by facet reflections.⁷ Applying low enough anti-reflection coating is challenging but we circumvented this by implementing a chip geometry preventing reflection from facet(s). Our approach enables high power operation even in the absence of anti-reflection coatings.

The SLD structure was grown using molecular beam epitaxy (MBE) on an n-type GaSb substrate. It comprised a 200 nm thick GaSb buffer layer, a 2700 nm n-doped Al_{0.5}GaAsSb cladding layer, two compressively strained 10 nm GaIn_{0.22}Sb QWs embedded in 280 nm Al_{0.3}GaAsSb waveguide layers, a 2000 nm p-doped cladding layer, and a highly p-doped 200 nm GaSb contact layer.

After the MBE growth, the wafer was processed into ridge waveguide (RWG) devices. To ensure transverse single-mode operation, we studied different ridge widths and selected those with a suitable far-field profile. The best performance was obtained with a ridge width 5 μm and the etching depth 1900 nm. Ridge patterns were defined on a SiO₂ hard mask by employing UV-lithography and dry etching. The patterns were then transferred to the semiconductor by inductively coupled plasma (ICP) etching with Cl₂/N₂. After the ridge etching, the SiO₂ hard mask was removed by another RIE step followed by a plasma-enhanced chemical vapor deposition (PECVD) of SiN to act as an insulator. The contact window on top of the ridge was opened by RIE-etching the SiN, and a p-side Ti/Pt/Au Ohmic contact was deposited using e-beam evaporation. Afterwards, the wafer was thinned down to about 140 μm and the back side Ni/Au/Ge/Au contact was evaporated on the samples. For measurements, the wafer was cleaved into chips of different lengths. Finally, devices were mounted on AlN-ceramic submounts that were soldered to copper heatsinks.

^{a)} Author to whom correspondence should be addressed. Electronic mail: nouman.zia@tut.fi

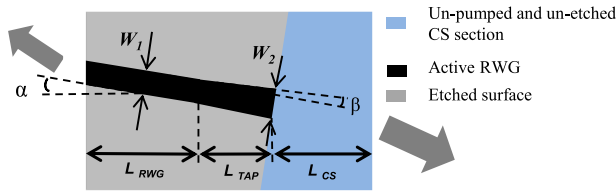


FIG. 1. Schematic drawing of the SLD waveguide geometry. The cavity suppression (CS) element is on the right hand side of the picture.

In order to prevent the lasing inside the cavity, different approaches have been reported, e.g., tilting the RWG at an angle (α) to the chip facets,¹⁰ adding a passive absorption section at one end of the waveguide,¹¹ or a combination of different approaches.¹² In this work, we etched the RWG at a 7° angle with respect to the cavity facets for achieving a low modal reflectivity.^{9,13} Although a larger angle can give low reflectivity, it will reduce the output beam coupling because of a larger beam exit angle. The cavity oscillations were further suppressed by defining a non-index guided region at the one-end of the chip; i.e., by preventing etching of the ridge waveguide at that end. To avoid current injection into the non-index guided end of the chip, this section was covered with the dielectric before metallization. However, we expect some longitudinal current leakage from the gain section to the cavity suppression (CS) section. The CS section provides some absorption but it also prevents light from reflecting back to the waveguide and thus from contributing to the cavity resonance. To avoid an abrupt change in the effective refractive index for the fundamental transverse mode exiting from the transversely confined gain section, the waveguide was slightly tapered at the interface between the two sections. This was to ensure that the beam exiting into the cavity suppression element does not reflect back due to a change in the effective refractive index. No antireflection (AR) or other coatings were applied to the facets of these devices. The schematic of the above-described device is shown in Fig. 1 with corresponding geometrical parameters in Table I.

It is clear from the device geometry shown in Fig. 1 that the output beam from the facet with the CS-element will experience astigmatism¹⁴ due to the fact that the emission along the slow axis and the fast axis originates from two different point-like sources. In the application of the SLDs, the astigmatism influences the focusing and collimation optics required after the light source. Therefore, the measurement¹⁵ and correction of the astigmatism are critical to have a well

TABLE I. Parameters of the SLD geometry shown in Fig. 1.

| Parameter | Value |
|--|-------|
| RWG length L_{RWG} (μm) | 2850 |
| CS length L_{CS} (μm) | 150 |
| RWG width W_1 (μm) | 5 |
| Tapered width W_2 (μm) | 10 |
| Tapered length L_{TAP} (μm) | 125 |
| Tilt angle α ($^\circ$) | 7 |
| Tapered angle β ($^\circ$) | 1 |

collimated or focused beam. Correction can be done in several ways, e.g., by using collimators¹⁶ or an anamorphic gradient-index lens.¹⁴

The SLDs have been characterized at room temperature by measuring power-current-voltage (L-I-V) characteristics (using a photodiode), far-fields (using a scanning goniometer, Nanofoot FFPnano), and spectrum (Yokogawa AQ6375 optical spectrum analyzer). Fig. 2(a) shows the CW power measured from CS and non-CS facets of the SLD as a function of current. The output power in Fig. 2 increases super-linearly up to a few mW showing amplified spontaneous emission (ASE). At larger currents, the output power increases sub-linearly due to gain saturation. It is important to note that the power emitted from the facet with the CS-element is significantly higher than that from the other facet. This power difference is due to the partial light reflection from the non-CS-element facet that exhibits double pass gain while nearly all light exiting from the non-CS-element facet experiences only single pass gain. The maximum optical power achieved by the SLD, without any heatsink, is 48 mW at 1200 mA, which is limited by self-heating at high currents. Therefore, the device was mounted on a heatsink, which increased the maximum power up to 60 mW from the CS facet, as shown in Fig. 2(b).

The spectral emission for the SLD is shown in Fig. 3, revealing fairly broad emission spectra with 60–70 nm FWHM which, together with the L-I curve reported in Fig. 2, is clear evidence of superluminescence in our device. Smoothness of the spectrum is quantified by the measurement of the spectral modulation (SM) that maps the difference between intensity minima I_{\min} and maxima I_{\max} as a function of the wavelength, i.e., $SM = (I_{\max} - I_{\min}) / (I_{\max} + I_{\min})$. A SM value of 0.035 was estimated for a corresponding current of 1 A. Such a low value for SM is evidence of the low modal reflectivity owing to the cavity design employed. We can notice an increase in the spectral width of the SLD with increasing current, which may be attributed to the rapid increase in the material gain bandwidth,¹⁷ because

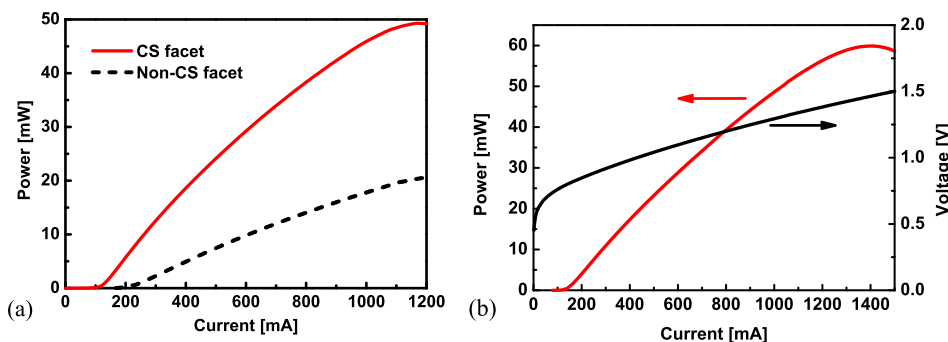


FIG. 2. (a) L-I curve for a fabricated SLD, at RT and CW operation, when measured without heatsink from CS and non-CS facets; (b) L-I-V characteristic for a SLD mounted on a heatsink.

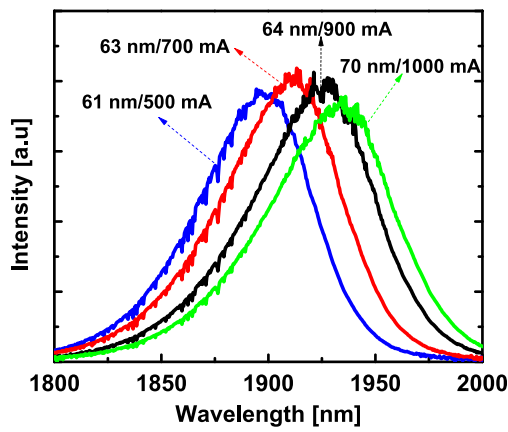


FIG. 3. SLD emission spectra measured at different currents. Arrows indicate the FWHM of the spectrum at injected current.

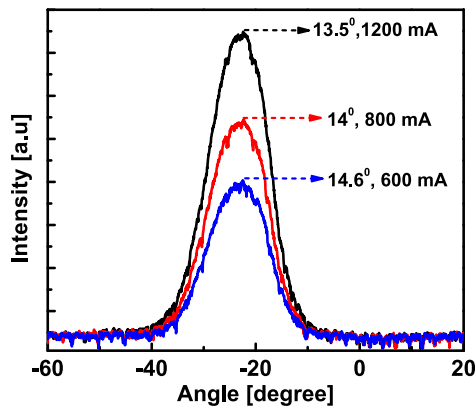


FIG. 4. SLD slow axis far-field with different injection currents. Arrows indicate the FWHM of far-field at injected current.

the carrier density in the active region is increasing rapidly. With an increasing current, there is a redshift of about 80 nm/A in the spectra due to the self-heating of the device, which causes bandgap shrinkage.¹⁸ Therefore, it can be concluded that gain saturation mentioned before can be due to heating effects.

Far-field, from the CS-facet, measured along the slow axis, shown in Fig. 4 indicates operation in a single transverse mode without any side lobes. Such performance shows the ability of these devices to efficiently couple light in a single mode optical fiber. A shift of 23° in the far-field is due to the tilt of RWG, which can be obtained from Snell's law.

In conclusion, we have demonstrated electrically pumped high power, single transverse mode SLDs operated at RT in CW. These devices produced a power of 60 mW and have broad and smooth spectra with 60 nm FWHM centered around the wavelength 1.9 μm. These characteristics are attributed to implementation of a waveguide geometry that includes a tilted RWG with a passive transversely unguided section. The transverse mode operation and the waveguide geometry meet the requirements for hybrid integration with passive silicon waveguides opening opportunities for demonstrating photonic integrated circuits at mid-IR wavelengths, with many applications in spectroscopy.

The authors wish to acknowledge funding from project European Union Horizon 2020 project MIREGAS "Programmable multi-wavelength Mid-IR source for gas sensing," Contract No. 644192. S. Suomalainen wishes to thank also Academy of Finland (project NANoS, Project No. 260815) for personal financial support. In addition, authors are grateful to Ms. Mervi Koskinen for her help in the semiconductor processing.

- ¹L. S. Rothman, I. E. Gordon, A. Barbe, D. C. Benner, P. F. Bernath, M. Birk, V. Boudon, L. R. Brown, A. Campargue, J.-P. Champion *et al.*, "The HITRAN 2008 molecular spectroscopic database," *J. Quant. Spectrosc. Radiat. Trans.* **110**, 533 (2009).
- ²S. Sprengel, C. Grasse, K. Vizbaras, T. Gruendl, and M.-C. Amann, "Up to 3 μm light emission on InP substrate using GaInAs/GaAsSb type-II quantum wells," *Appl. Phys. Lett.* **99**(22), 221109 (2011).
- ³T. Hosoda, T. Feng, L. Shterengas, G. Kipshidze, and G. Belenky, "High power cascade diode lasers emitting near 2 μm," *Appl. Phys. Lett.* **108**, 131109 (2016).
- ⁴J. Viheriälä, K. Haring, S. Suomalainen, R. Koskinen, T. Niemi, and M. Guina, "High spectral purity high-power GaSb-based DFB laser fabricated by nanoimprint lithography," *IEEE Photonics Technol. Lett.* **28**(11), 1233 (2016).
- ⁵C. Lin, M. Grau, O. Dier, and M.-C. Amann, "Low threshold room-temperature continuous-wave operation of 2.24-3.04 μm GaInAsSb/AlGaAsSb quantum-well lasers," *Appl. Phys. Lett.* **84**, 5088 (2004).
- ⁶D. S. Mamedov, V. V. Prokhorov, and S. D. Yakubovich, "Broadband radiation sources based on quantum-well superluminescent diodes emitting at 1550 nm," *Quantum Electron.* **33**(11), 511 (2003).
- ⁷M. B. Wooten, J. Tan, Y. J. Chien, J. T. Olesberg, and J. P. Prineas, "Broadband 2.4 μm superluminescent GaInAsSb/AlGaAsSb quantum well diodes for optical sensing of biomolecules," *Semicond. Sci. Technol.* **29**, 115014 (2014).
- ⁸C. Grasse, T. Gruendl, S. Sprengel, P. Wiecha, K. Vizbaras, R. Meyer, and M.-C. Amann, "GaInAs/GaAsSb-based type-II micro-cavity LED with 2–3 μm light emission grown on InP substrate," *J. Cryst. Growth* **370**, 240 (2013).
- ⁹K. Vizbaras, E. Dvinelis, I. Šimonytė, A. Trinkūnas, M. Greibus, R. Songaila, T. Žukauskas, M. Kaušlyas, and A. Vizbaras, "High power continuous-wave GaSb-based superluminescent diodes as gain chips for widely tunable laser spectroscopy in the 1.95-2.45 μm wavelength range," *Appl. Phys. Lett.* **107**, 011103 (2015).
- ¹⁰G. A. Alphonse, "Design of high-power superluminescent diodes with low spectral modulations," *Proc. SPIE* **4648**, 125 (2002).
- ¹¹A. Kafar, S. Stańczyk, R. Czernecki, M. Leszczyński, T. Suski, and P. Perlin, "Cavity suppression in nitride based superluminescent diodes," *J. Appl. Phys.* **111**, 083106 (2012).
- ¹²T. Yamatoya, S. Sekiguchi, F. Koyama, and K. Iga, "High-power CW operation of GaInAsP/InP superluminescent light-emitting diode with tapered active region," *Jpn. J. Appl. Phys., Part 2* **40**, L678 (2001).
- ¹³G. A. Alphonse and M. Toda, "Mode coupling in angled facet semiconductor optical amplifiers and superluminescent diodes," *J. Lightwave Technol.* **10**, 215 (1992).
- ¹⁴E. Acosta, R. M. Gonzalez, and C. Gomez-Reino, "Design of an anamorphic gradient-index lens to correct astigmatism of Gaussian laser beams," *Opt. Lett.* **16**, 627 (1991).
- ¹⁵W. D. Herzog, M. S. Ünlü, B. B. Goldberg, and G. H. Rhodes, "Beam divergence and waist measurement of laser diodes by near field scanning optical microscopy," *Appl. Phys. Lett.* **70**, 688 (1997).
- ¹⁶M. Lang, "Correcting astigmatism in diode lasers," *Laser Optron.* **8**(9), 51 (1989).
- ¹⁷J. Park and X. Li, "Theoretical and numerical analysis of superluminescent diodes," *J. Lightwave Technol.* **24**(6), 2473 (2006).
- ¹⁸A. Tomita and A. Suzuki, "Carrier-induced lasing wavelength shift for quantum well laser diodes," *IEEE J. Quantum Electron.* **23**, 1155 (1987).